

# Synthesis of Nitrogen-Containing Microporous Carbon with a Highly Ordered Structure and Effect of Nitrogen Doping on H<sub>2</sub>O Adsorption

Peng-Xiang Hou,<sup>†</sup> Hironori Orikasa,<sup>†</sup> Toshiaki Yamazaki,<sup>†</sup> Koichi Matsuoka,<sup>†</sup>  
Akira Tomita,<sup>†</sup> Norihiko Setoyama,<sup>‡</sup> Yoshiaki Fukushima,<sup>‡</sup> and Takashi Kyotani<sup>\*,†</sup>

*Institute of Multidisciplinary Research for Advanced Materials, Tohoku University, 2-1-1 Katahira, Aoba-Ku, Sendai 980-8577, Japan, and Toyota Central Research and Development Laboratory, Incorporated, Nagakute, Aichi 480-1192, Japan*

*Received May 22, 2005. Revised Manuscript Received August 1, 2005*

A nitrogen-containing microporous carbon with a highly ordered structure was synthesized by using zeolite Y as a template. The filling of carbon into zeolite channels was performed by the impregnation of furfuryl alcohol and subsequent chemical vapor deposition (CVD) of acetonitrile. The template was then removed by HF washing. The two-step carbon filling process (the impregnation and the CVD) was found to be essential for obtaining both high microporosity and ordering. This carbon is characterized by its very large surface area (3310 m<sup>2</sup>/g) and very narrow micropore size distribution (1.0–1.5 nm), and it contains nitrogen of 6 wt %, most of which is quaternary nitrogen. The distribution of nitrogen atoms in the carbon was examined by the detailed analysis of the carbon deposit at each carbon-filling step. The effect of nitrogen doping on the affinity to H<sub>2</sub>O molecules was elucidated from the comparison of the H<sub>2</sub>O adsorption behavior between this carbon and a nitrogen-free ordered porous carbon with a very similar pore structure. It was found that the nitrogen-containing carbon has a higher affinity to H<sub>2</sub>O molecules than the nitrogen-free carbon.

## Introduction

Porous carbons have gathered more and more attention because they hold great potential for applications in gas storage,<sup>1</sup> as the electrodes of electric double-layer capacitors,<sup>2</sup> and for environmental technologies such as the removal of pollutants.<sup>3,4</sup> The investigation of nitrogen (N) present in carbonaceous materials has been a subject of considerable research efforts for the past two decades. This research was performed partially for minimizing the negative impact on the environment due to the formation and emission of nitrous and nitric oxides during the combustion of coal. On the other hand, some other researches have paid attention to N-containing porous carbons because the introduction of N atoms endows the carbons with a polar nature. Their physicochemical properties would thus be different from those of N-free porous carbons and are more desirable for the application to the electrodes of electric double-layer capacitors.<sup>5,6</sup>

Porous carbons containing N atoms can be obtained using the following several methods: (1) reaction of porous carbons with N-containing gases;<sup>7–9</sup> (2) cocarbonization of N-free and N-containing precursors;<sup>10–12</sup> and (3) carbonization of raw material containing N atoms.<sup>13</sup> However, due to the complexity of the carbon pore structure, it is very difficult to tailor their pore structure, especially their microporosity. It is well-known that the degree of microporosity is an essential factor affecting the performance of porous carbons in many applications. The control of both micropore size and micropore–wall chemistry is, therefore, indispensable for further improvement of the performance, but such control is a very difficult task.

The template method is a promising approach to control the carbon pore structure.<sup>14</sup> Using a variety of inorganic porous templates, so far many researchers have prepared novel porous carbons including N-containing mesoporous carbons.<sup>15–22</sup> We prepared a long-range ordered microporous

\* Corresponding author. Phone: +81-22-217-5625. Fax: +81-22-217-5626. E-mail: kyotani@tagen.tohoku.ac.jp.

<sup>†</sup> Tohoku University.

<sup>‡</sup> Toyota Central Research and Development Laboratory, Incorporated.

- (1) Norman, D. P.; David, F. Q. In *Porosity in Carbons*; Patrick, J. W., Ed.; John Wiley: New York, 1995; p 292.
- (2) Frackowiak, E.; Beguin, F. *Carbon* **2001**, *39*, 937.
- (3) Raymundo-Pinero, E.; Cazorla-Amorós, D.; Linares-Solano, A. *Carbon* **2003**, *41*, 1925.
- (4) Mochida, I.; Kawano, S.; Shirahama, N.; Enjoji, T.; Moon, S. H.; Sakanishi, K.; Korai, Y.; Yasutake, A.; Yoshikawa, M. *Fuel* **2001**, *80*, 2227.
- (5) Kodama, M.; Yamashita, J.; Soneda, Y.; Hatori, H.; Nishimura, S.; Kamegawa, K. *Mater. Sci. Eng. B* **2004**, *108*, 156.

- (6) Hulicova, D.; Yamashita, J.; Soneda, Y.; Hatori, H.; Kodama, M. *Chem. Mater.* **2005**, *17*, 1241.
- (7) Stöhr, B.; Boehm, H. P.; Schlögl, R. *Carbon* **1991**, *29*, 707.
- (8) Jansen, R. J. J.; van Bekkum, H. *Carbon* **1994**, *32*, 1507.
- (9) Yang, C. M.; El-Merraoui, M.; Seki, H.; Kaneko, K. *Langmuir* **2001**, *17*, 675.
- (10) Singoredjo, L.; Kapteijn, F.; Moulijn, J. A.; Martin-Martinez, J. M.; Boehm, H. P. *Carbon* **1993**, *31*, 213.
- (11) Raymundo-Pinero, E.; Cazorla-Amorós, D.; Linares-Solano, A.; Find, J.; Wild, U.; Schlögl, R. *Carbon* **2002**, *40*, 597.
- (12) Machnikowski, J.; Grzyb, B.; Weber, J. V.; Frackowiak, E.; Rouzaud, J. N.; Béguin, F. *Electrochim. Acta* **2004**, *49*, 423.
- (13) Lahaye, J.; Nansé, G.; Bagreev, A.; Strelko, V. *Carbon* **1999**, *37*, 585.
- (14) Kyotani, T. *Carbon* **2000**, *38*, 269.
- (15) Gilbert, M. T.; Knox, J. H.; Kaur, B. *Chromatographia* **1982**, *16*, 138.
- (16) Pekala, R. W.; Hopper, R. W. *J. Mater. Sci.* **1987**, *22*, 1840.

carbon with a structural regularity of zeolite Y for the first time.<sup>23–25</sup> This porous carbon possesses a high BET specific surface area more than 3000 m<sup>2</sup>/g and almost no mesoporosity. Furthermore, its pore size distribution is very narrow in comparison with commercial high surface area carbons, and most of the pore sizes are in the range of 1.0–1.5 nm.<sup>26</sup> Very recently, Su and co-workers used NH<sub>4</sub>-form zeolite Y as a template to prepare microporous carbons from poly-(furfuryl alcohol) and found that the resulting carbons contained N of 2–7 wt %.<sup>27</sup> However, the regularity of zeolite Y was not reflected in the carbon structure, and the pore size distribution was somewhat broad as a result. The presence of the regularity in the carbon structure is essential for obtaining such narrow micropore size distribution as observed in our previous study.<sup>26</sup>

In the present study, we try to synthesize N-containing microporous carbons having both the regularity of zeolite Y and monodispersed pore size distribution. Moreover, we compare the adsorption behavior of H<sub>2</sub>O molecules on the N-containing microporous carbons with that on the N-free microporous carbon prepared previously and thereby elucidate the effect of N doping on the H<sub>2</sub>O adsorption.

### Experimental Procedures

**Synthesis.** A two-step method was applied in the preparation of N-containing microporous carbons. In the first step, the nanochannels of zeolite Y (Na-form, SiO<sub>2</sub>/Al<sub>2</sub>O<sub>3</sub> = 5.6, Tosoh Inc., HSZ-320NAA) were filled with furfuryl alcohol by an impregnation method, and then furfuryl alcohol was polymerized at 150 °C. The resulting poly(furfuryl alcohol) (PFA)/zeolite composite was placed in a vertical quartz reactor (20 mm i.d.) and heated to a predetermined temperature (700, 800, or 900 °C) under N<sub>2</sub> flow at a heating rate of 5 °C/min to carbonize the PFA in the composite. The second step was chemical vapor deposition (CVD) of acetonitrile over the zeolite composite. As soon as the reactor reached one of the previous temperatures just after the first step, acetonitrile vapor (4.2% in N<sub>2</sub> of 150 cm<sup>3</sup> (STP)/min) was introduced into the reactor. The vapor was generated by bubbling N<sub>2</sub> through acetonitrile liquid in a saturator at 0 °C. This acetonitrile CVD was performed for a given time (1, 2, 3, or 4 h), and then the composite was further heat-treated at 900 °C under N<sub>2</sub> flow for 1 h. Finally, the carbon part was liberated from the zeolite framework by HF washing. The stability of the zeolite framework structure at 900 °C was confirmed by the XRD measurement of the carbon/zeolite composites. In the present study, we mainly changed CVD temperature and time and investigated the effect of these parameters on the structure of the resulting porous carbons. For convenience,

the acetonitrile CVD conditions are indicated through this paper as AX(Y), where the X following the A (meaning acetonitrile CVD) denotes one hundredth of the CVD temperature (in °C) and the Y in parentheses corresponds to the CVD time in hours. For example, A8(2) means the acetonitrile CVD at 800 °C for 2 h.

To investigate the necessity for the first step, we intentionally skipped the first step in some of the experimental runs. In other words, we tried to prepare N-containing carbons only with the CVD without the furfuryl alcohol impregnation. This method is identified with an asterisk. For example, A8(2)\* denotes acetonitrile CVD at 800 °C for 2 h but without furfuryl alcohol impregnation. Furthermore, to examine the effect of N introduction, we prepared an N-free carbon having a similar type of microporous structure by the two-step method but using propylene as carbon source in the CVD process (at 700 °C for 1 h). This process is referred to as P7(1) hereafter. Some of the P7(1) composite powders were subjected to further CVD using acetonitrile at 800 °C for 0.5 h. This two-CVD process is referred to as P7(1)–A8(0.5). Finally, the heat-treatment at 900 °C in N<sub>2</sub> and the subsequent HF washing were performed for all these carbon/zeolite composites.

**Characterization.** The structure of the resulting carbons was examined using an X-ray diffractometer (XRD, Shimadzu, XD-D1) with Cu K $\alpha$  radiation. The N-content and types of N-functionalities in the carbons were determined with elemental analysis and X-ray photoelectron spectroscopy (XPS), respectively. In the latter analysis, the powdered samples were placed on a stainless steel sample holder with electroconductive carbon adhesive tape. Nitrogen 1s (N<sub>1s</sub>) and C<sub>1s</sub> spectra were recorded using a PHI 5600 ESCA spectrometer with Mg K $\alpha$  radiation (8 kV, 30 mA) under a pressure of less than 10<sup>–6</sup> Pa at different photoelectron takeoff angles (from 15 to 75°) relative to the top surface of the sample holder. A binding energy correction was made to account for sample charging based on a C<sub>1s</sub> peak at 284.6 eV. The microscopic features of the carbons were observed with a scanning electron microscope (SEM, JEOL SM71010) and a transmission electron microscope (TEM, JEOL JEM-2010). The specific surface area and pore structure of the samples were investigated with an automatic volumetric sorption analyzer (Quantachrome, Autosorb-1) using N<sub>2</sub> as the adsorbate at –196 °C. The BET specific surface areas of all the samples were determined using the data in the relative pressure range of 0.01–0.05, as recommended by Kaneko et al.<sup>28</sup> for analyzing porous carbons with very high surface areas. The micropore volume was calculated from the Dubinin–Radushkevich (DR) equation. The mesopore volume was determined by subtracting the micropore volume from the volume of N<sub>2</sub> adsorbed at a relative pressure ( $P/P_0$ ) of 0.95. For some of the carbons, the pore size distribution was estimated using the N<sub>2</sub> adsorption isotherm based on the density functional theory (DFT) method, which is available in the Autosorb software (Quantachrome). Sorption isotherms of H<sub>2</sub>O at 25 °C were obtained using a volumetric water vapor adsorption apparatus (Belsorp-18; BEL Japan). Prior to the H<sub>2</sub>O adsorption tests, the samples were outgassed at 110 °C for 6 h under vacuum less than 1 Pa.

### Results and Discussion

**Optimum Condition for Synthesizing Ordered N-Containing Porous Carbons.** To investigate an optimum synthesis condition to achieve both high regularity and microporosity, we varied mainly the CVD conditions (temperature and period) and evaluated the resulting carbons from the results of the XRD and N<sub>2</sub>-adsorption measurements. At

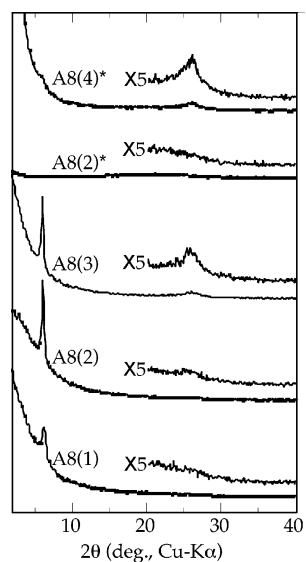
- 
- (17) Kyotani, T.; Nagai, T.; Inoue, S.; Tomita, A. *Chem. Mater.* **1997**, *2*, 6609.  
(18) Zakhidov, A. A.; Baughman, R. H.; Iqbal, Z.; Cui, C. X.; Khayrullin, I.; Dantas, S. O.; Marti, J.; Ralchenko, V. G. *Science* **1998**, *282*, 897.  
(19) Ryou, R.; Joo, S. H.; Jun, S. *J. Phys. Chem. B* **1999**, *103*, 7743.  
(20) Lee, J.; Yoon, S.; Hyeon, T.; Oh, S. M.; Kim, K. B. *Chem. Commun.* **1999**, *21*, 2177.  
(21) Lu, A. H.; Kiefer, A.; Schmidt, W.; Schüth, F. *Chem. Mater.* **2004**, *16*, 100.  
(22) Xia, Y.; Yang, Z.; Mokaya, R. *J. Phys. Chem. B* **2004**, *108*, 19293.  
(23) Ma, Z. X.; Kyotani, T.; Tomita, A. *Chem. Commun.* **2000**, *23*, 2365.  
(24) Ma, Z. X.; Kyotani, T.; Liu, Z.; Terasaki, O.; Tomita, A. *Chem. Mater.* **2001**, *13*, 4413.  
(25) Ma, Z. X.; Kyotani, T.; Tomita, A. *Carbon* **2002**, *40*, 2367.  
(26) Matsuoka, K.; Yamagishi, Y.; Yamazaki, T.; Setoyama, N.; Tomita, A.; Kyotani, T. *Carbon* **2005**, *43*, 876.  
(27) Su, F.; Zhao, X. S.; Lv, L.; Zhou, Z. *Carbon* **2004**, *42*, 2821

- 
- (28) Kaneko, K.; Ishii, C. *Colloid Surf.* **1992**, *67*, 203.

**Table 1. Specific Surface Area and Pore Volumes of Carbons Prepared under Different CVD Conditions**

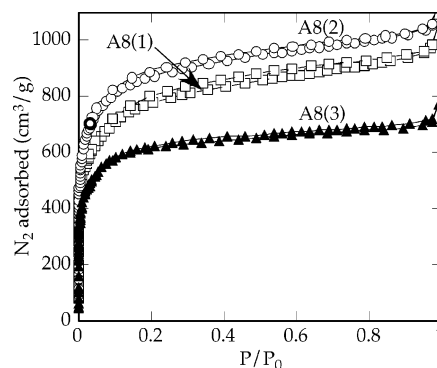
samples	CVD conditions			SBET <sup>a</sup> (m <sup>2</sup> /g)	V <sub>micro</sub> <sup>b</sup> (cm <sup>3</sup> /g)	V <sub>meso</sub> <sup>c</sup> (cm <sup>3</sup> /g)	V <sub>microH<sub>2</sub>O</sub> <sup>d</sup> (cm <sup>3</sup> /g)
	gas	temp. (°C)	time (h)				
A8(1)	acetonitrile	800	1	2880	1.06	0.50	n.d. <sup>e</sup>
A8(2)	acetonitrile	800	2	3310	1.26	0.33	1.23
A8(3)	acetonitrile	800	3	2260	0.91	0.49	n.d.
A8(2) <sup>*f</sup>	acetonitrile	800	2	1080	0.42	0.33	n.d.
A8(4) <sup>*f</sup>	acetonitrile	800	4	990	0.38	0.40	n.d.
P7(1)	propylene	700	1	4070	1.78	0.23	1.76
P7(1)–A8(0.5)	propylene,	700	1	3410	1.35	0.11	1.33
	acetonitrile	800	0.5				

<sup>a</sup> BET specific surface area determined using the data at  $P/P_0 = 0.01–0.05$ . <sup>b</sup> Micropore volume from DR eq. <sup>c</sup> By subtracting the micropore volume from the volume of N<sub>2</sub> adsorbed at  $P/P_0 = 0.95$ . <sup>d</sup> Micropore volume from H<sub>2</sub>O adsorption isotherm. <sup>e</sup> Not determined. <sup>f</sup> The asterisk means that the furfuryl alcohol impregnation process was skipped and that only the CVD process was performed.

**Figure 1.** X-ray diffraction patterns of the carbons synthesized under the acetonitrile CVD at 800 °C.

first, we focused on whether an XRD peak appeared around 6° or not. The peak originates from the ordering of {111} planes of zeolite Y, and the presence of this peak can be used as a measure of the regularity in the resulting carbon structure. It was found that such an XRD peak was observed for every carbon sample synthesized under the CVD at 800 °C (Figure 1), whereas for the samples under CVD at 700 and 900 °C, no peak or a very weak one was detected (not shown here). Among A8 carbons, the CVD times for 2 and 3 h resulted in higher ordering than the shorter one (1 h), based on the sharpness and intensity of their XRD peaks in Figure 1. The A8(3) carbon, however, gives not only the sharp XRD peak but also the broad peak in the range of 20–30°, which can be ascribed to the diffraction from carbon layer stacking of the deposits on the external surface of zeolite particles as suggested by Ma et al.<sup>25</sup> The presence of such broad diffraction therefore indicates that the carbon deposition took place not only in the nanochannels of zeolite particles but also on their external surface. The latter type of deposition should be avoided as much as possible for obtaining porous carbons with a highly ordered structure. The previous results thus suggest that CVD should not be performed for as long a period as 3 h.

The porosity of the synthesized carbons was analyzed by N<sub>2</sub> adsorption at –196 °C. The adsorption–desorption isotherms of A8 carbons are plotted in Figure 2, and the results of the specific surface areas and the pore volumes

**Figure 2.** N<sub>2</sub> adsorption–desorption isotherms of the carbons (–196 °C).**Table 2. Results of Elemental Analysis for Carbons**

samples	elemental analysis (wt %)			
	C	H	N	O (diff.)
A8(1)	86	3	4	7
A8(2)	88	2	6	4
A8(3)	89	1	7	3
A8(2) <sup>*</sup>	83	3	5	9
A8(4) <sup>*</sup>	87	2	7	4
P7(1)	90	2	0	8
P7(1)–A8(0.5)	91	2	2	5

are summarized in Table 1. Their N<sub>2</sub> adsorption isotherms are of Type I, suggesting the microporous nature of these carbons. Among them, A8(2) carbon has the largest surface area and micropore volume (3310 m<sup>2</sup>/g and 1.26 cm<sup>3</sup>/g) and the smallest mesopore volume (0.33 cm<sup>3</sup>/g). The previous results reveal that the acetonitrile–CVD condition (800 °C and 2 h) is an optimum for synthesizing porous carbon having a high specific surface area and high microporosity. Interestingly, this optimum CVD condition is the same as that for obtaining porous carbon with highly structural regularity judging from the XRD results. A sharp peak around 6° in an XRD pattern is therefore a simple criterion for the synthesis of porous carbon with a large surface area and high microporosity.

We can conclude that there is an optimum CVD condition for synthesizing a highly ordered microporous carbon. In the present work, the CVD for 2 h at 800 °C (A8(2)) is the best one. The elemental analysis results (Table 2) of this carbon confirm the presence of N, and its ash content (nearly zero) indicates complete removal of the zeolite template. In the two-step method, the furfuryl alcohol impregnation was always performed before the CVD process. Since PFA does not contain any nitrogen, it would be better to avoid this impregnation process, if possible, for obtaining a porous

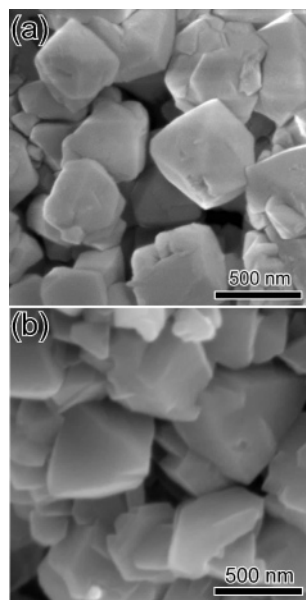


**Figure 3.** SEM images of zeolite Y (a) and A8(2) carbon (b).

carbon with a large content of N. To check the effect of PFA, we prepared two types of porous carbons without this impregnation process but only with the CVD at 800 °C for 2 and 4 h (A8(2)\* and A8(4)\*). It was found that both carbons had no XRD peak around 6° (Figure 1) and possessed much less specific surface area and micropore volume than the carbon prepared with the two-step method (Table 1), indicating that the presence of PFA before the acetonitrile CVD is indispensable to develop both regularity and microporosity. Surprisingly, the N content for these two carbons is not as large as expected, but it is comparable to that for the other carbons synthesized with the two-step method (Table 2). We have no clear explanation for this phenomenon, but the already-existing PFA-derived substance might influence the subsequent acetonitrile CVD behavior.

#### Analysis of the Ordered N-Containing Porous Carbon.

As described previously, A8(2) carbon possesses the most ordered and microporous structure so that more detailed analyses were carried out for this carbon. Figure 3 shows SEM images of A8(2) carbon and the parent zeolite. The SEM image of zeolite Y (Figure 3a) exhibits crystal habits in each particle with a size of about 500 nm, indicating that each one almost corresponds to a single crystal and/or consists of a few single crystals. The crystal face of the original zeolite particles is clearly reflected in the smooth surface of the carbon particles (Figure 3b). As already reported in the previous paper,<sup>25</sup> when serious carbon deposition on the external surface of zeolite particles took place, the surface of the carbon particles liberated from such composites looked rough in comparison with the smooth surface of zeolite particles. The presence of such a smooth surface on the A8(2) carbon particles suggests that the acetonitrile CVD process (A8(2)) deposited carbon mostly inside the zeolite channels and that the deposition on the external surface was not remarkable. The presence of carbon inside the particles was confirmed by a low-magnification TEM image of this sample (Figure 4a), where several carbon particles with a size of about 500 nm are observed. Figure 4b shows a high-magnification TEM image of a part of one

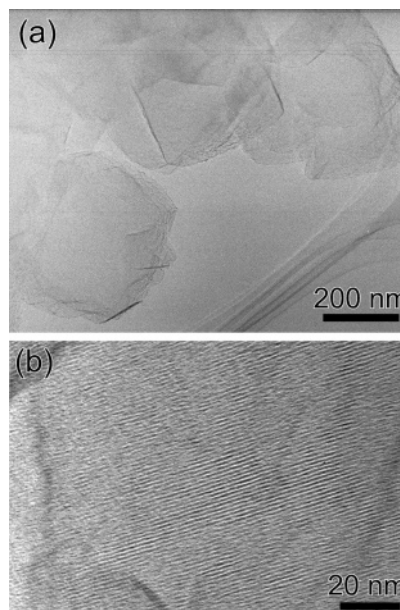


**Figure 4.** TEM images of A8(2) carbon: (a) a low-magnification image of carbon particles and (b) a high-resolution image of a part of one carbon particle.

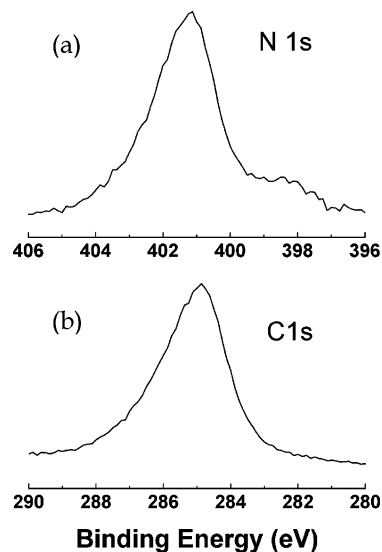


**Figure 5.** X-ray photoelectron  $N_{1s}$  and  $C_{1s}$  spectra of A8(2) carbon.

carbon particle. From the image, straight lattice fringes can readily be seen, and the regular spacing of the observed lattice planes is about 1.3 nm, which is in good agreement with the ordering (about 1.39 nm) determined from the XRD measurement. The observation of such ordering is other solid evidence for the presence of the regularity in A8(2) carbon.

As revealed by the elemental analysis, N atoms have been introduced into this porous carbon (Table 2). To clarify the chemical circumstance of N in A8(2) carbon, its surface was investigated with XPS at a takeoff angle of 45°. The resulting  $N_{1s}$  spectrum is plotted in Figure 5a, where one distinct peak is observed at 401.2 eV with a shoulder around 398 eV. These can be attributed to quaternary and pyridinic N, respectively, and the former one is the main N-functionality in the present carbon. Pels<sup>29</sup> suggested that quaternary N may

(29) Pels, J. R.; Kapteijin, F.; Moulijn, J. A.; Zhu, Q.; Thomas, K. M. *Carbon* **1995**, *33*, 1641.

**Table 3. Carbon Fraction, Surface Area, and Pore Volume for Zeolite and Carbon/Zeolite Composites<sup>a</sup>**

samples	carbon fraction <sup>b</sup> (g/g of zeolite)	BET specific surface area <sup>c</sup> (m <sup>2</sup> /g)	pore volume <sup>d</sup> (cm <sup>3</sup> /g)
zeolite Y	0	870	0.37
zeolite Y + PFA carbon (before A8(2) CVD)	0.14	560	0.24
A8(2) composite (after A8(2) CVD)	0.25	11	0.03
P7(1) composite (after P7(1) CVD)	0.25	15	0.04

<sup>a</sup> All data were expressed per 1 g of zeolite. <sup>b</sup> Carbon fraction in each composite was calculated from the data of its elemental analysis using the carbon-to-ash ratio where ash was regarded as the zeolite equivalent. <sup>c</sup> Determined using the data at  $P/P_0 = 0.01-0.05$ . <sup>d</sup> Determined from the volume of N<sub>2</sub> adsorbed at  $P/P_0 = 0.95$ .

represent various forms, defined as more positively charged N, as compared to pyridinic-N, being part of a larger aromatic structure. This includes protonated pyridinic-N ammonium ions and N atoms replacing carbon atoms in graphene structures. The latter one is a more probable form for quaternary N in the present carbon.

In addition to the N<sub>1s</sub> spectrum, the XPS measurement for C<sub>1s</sub> was performed at the same angle as in the N<sub>1s</sub> measurement. The C<sub>1s</sub> spectrum is shown in Figure 5b, where a large peak is observed around 285 eV, which is attributed to the sp<sup>2</sup> carbon atoms of the carbon skeleton. This peak is broad on its high energy side (286–288 eV), and this shoulder indicates the presence of carbon atoms singly or doubly coordinated to an oxygen or nitrogen atom (C–O, C=O, C–N), but there is almost no carboxyl group because there is no clear XPS peak around 289 eV where the carboxyl group usually gives a peak. The area ratio of N<sub>1s</sub> to C<sub>1s</sub> signals corrected with standard XPS sensitivity factors can approximately be regarded as a surface atomic ratio of N to C for A8(2) carbon. In this study, this ratio was examined at different takeoff angles. It is well-known that the analysis depth of XPS is dependent on the takeoff angle and thus a study of takeoff angle dependence provides information about the surface depth profile. The N/C ratios determined at an angle of 15, 30, 45, 60, and 75° were found to be 0.061, 0.067, 0.065, 0.065, and 0.063, respectively. There is almost no change in the ratio with an increase in the angle, suggesting a uniform N depth profile at least in the surface layer that the present angle resolved XPS can detect. Furthermore, these values do not significantly differ from the bulk N/C ratio (0.058) determined from the elemental analysis. Considering that the present synthesis procedure consists of the two steps (the first impregnation of furfuryl alcohol into the zeolite channels and the subsequent CVD process using acetonitrile as N source), we could presume preferential N deposition on the outer surface of the carbon particles (Figure 3b) and hence could have obtained a much larger surface N/C ratio.

For further understanding of the N distribution in the carbon structure, we examined the porous nature of the carbon/zeolite composites before and after the acetonitrile CVD (A8(2)) by N<sub>2</sub> adsorption at –196 °C. The composite before CVD was prepared as follows: the PFA/zeolite composite was heat-treated up to 800 °C under exactly the same conditions as in the Experimental Procedures, and then the temperature was lowered as soon as it reached 800 °C. The composite after the CVD is just the A8(2) composite. From the resulting isotherms of these two composites, their BET specific surface area and pore volumes were determined, and they are summarized in Table 3 together with the data of the parent zeolite. In addition, carbon fraction in

each composite is indicated in the second column of the table. Although the zeolite channels were filled with furfuryl alcohol by the impregnation process, only a small amount of carbon (0.14 g/g of zeolite) remained due to the heat-treatment up to 800 °C. With each carbon-loading step (the PFA carbonization and then the acetonitrile CVD), the carbon fraction increases and the porosity decreases, as a matter of course. It should be noted that the composite before CVD still kept a relatively large porosity, but it was drastically reduced by the subsequent CVD. This finding suggests that many of the channels in the zeolite still remained open and unoccupied even after PFA carbonization, but such open and unoccupied channels were apparently occupied by N-containing carbon upon the next carbon-loading process (the acetonitrile CVD), as presumed from TEM images (Figure 4). In other words, N atoms were introduced to not only the outer surface of the particles but also their inside. This can explain why the difference in the N/C ratio between the surface and the bulk of A8(2) carbon was not large. However, considering the pore volume of the parent zeolite, we have to judge that the amount of carbon fraction (0.25 g/g of zeolite) is not enough for complete filling. It means that the composite still retains some open space, which N<sub>2</sub> molecules cannot access at as low a temperature as –196 °C. Furthermore, the small difference in the N/C ratio between the XPS measurements and the elemental analysis suggests that there is a slight heterogeneity in N distribution of the carbon substrate inside the zeolite.

**Two Reference Carbons for Comparison.** To investigate the effect of N doping, we compare A8(2) carbon with the N-free (P7(1)) carbon having a similar type of microporous structure. The details of P7(1) carbon were already reported elsewhere.<sup>26</sup> Briefly, the carbon fraction (0.25 g/g of zeolite) of the P7(1) composite is the same as that of the A8(2) one, and the P7(1) carbon does not contain any N, but its O content is twice as large as that of A8(2) (Table 2). XRD analysis revealed that P7(1) carbon showed a sharp peak around 6°, and its intensity and sharpness were almost the same as those of A8(2) carbon. We can thus presume that P7(1) carbon has an ordered structure similar to that of A8(2) carbon. The specific surface area and micropore and mesopore volumes of P7(1) carbon were determined in the same manner, and they are summarized in Table 1. The specific surface area of P7(1) reaches more than 4000 m<sup>2</sup>/g, and its micropore volume is as large as 1.8 cm<sup>3</sup>/g, each of which is larger than that of A8(2) carbon (i.e., P7(1) carbon is more microporous than A8(2)). In addition to P7(1) carbon, P7(1)–A8(0.5) carbon was also prepared for comparison. This carbon contains N of 2 wt % (Table 2) because the acetonitrile CVD (at 800 °C for 0.5 h, A8(0.5)) was performed after the propylene CVD (at 700 °C for 1 h, P7-

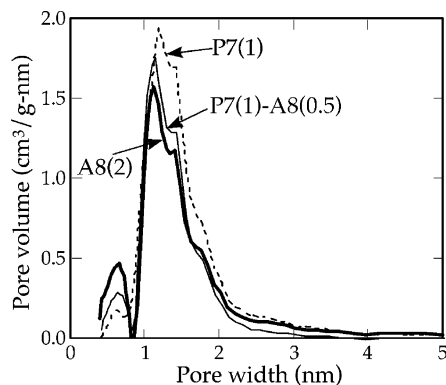


**Figure 6.** Pore size distribution curves determined by applying the DFT method to the  $N_2$  adsorption isotherms of the three carbons.

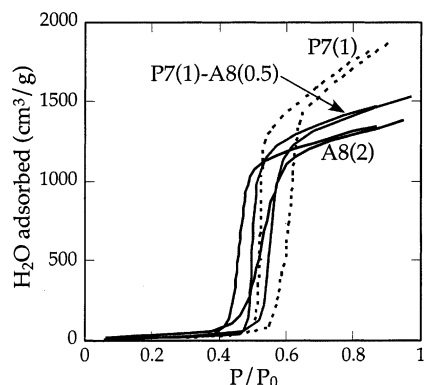


**Figure 7.**  $H_2O$  adsorption-desorption isotherms at 25 °C for the three types of carbons.

(1)). Its bulk N/C atomic ratio (0.019) is much smaller than the surface N/C ratio (0.040) determined from the XPS measurement. The carbon/zeolite composite before the acetonitrile CVD (i.e., P7(1) composite) has a very small surface area and pore volume (Table 3), indicating that most of the open channels were filled and/or plugged with N-free carbon. Nitrogen atoms introduced by the subsequent acetonitrile CVD (A8(0.5)) are distributed preferentially on the outer surface of the P7(1)-A8(0.5) carbon particles, as a result. The surface area and micropore volume of this carbon are smaller than those of P7(1) carbon but a little larger than those of A8(2) carbon (Table 1).

Despite the difference in microporosity among the three carbons, their pore size distribution (PSD) curves are similar, as demonstrated in Figure 6, where the three curves determined by the DFT method are illustrated. All of the carbons have a surprisingly sharp PSD curve, and most of the pore sizes fall within the range of 1.0–1.5 nm, which is comparable to a periodicity (1.4 nm) of the regularity in the three carbons. Such narrow PSD may be ascribed to the periodically ordered array structure of these carbons. The formation mechanism of the uniform micropores was described elsewhere.<sup>30</sup> All of these data here suggest that these carbons possess a very similar ordered microporous structure with a very narrow PSD.

**Role of N in  $H_2O$  Adsorption on Ordered Microporous Carbons.** The  $H_2O$  adsorption-desorption isotherms of the previous three carbons are plotted in Figure 7. Their

isotherms are of Type V, and the shape is characterized by a sharp adsorption uptake accompanied by a clear adsorption hysteresis occurring over a medium relative pressure ( $P/P_0$ ) range. Such characteristics have often been observed in  $H_2O$  isotherms of microporous carbons such as activated carbon fibers (ACF).<sup>31,32</sup> Mowla et al. found that the width of the hysteresis loop in  $H_2O$  isotherms for microporous carbons depends on their pore size; no hysteresis is observed for carbons with a pore size of less than 0.8 nm, but a wide loop exists for carbons having a larger pore size.<sup>33</sup> The latter is indeed the case for the present three carbon samples.

Because of the large micropore volumes of these carbons, the amounts of  $H_2O$  adsorbed are very large. For instance, the saturated amounts, determined by the extrapolation of each adsorption isotherm to  $P/P_0 = 1$ , are as large as 1.6, 1.2, and 1.1 g/g for P7(1), P7(1)-A8(0.5), and A8(2) carbons, respectively. From these values, the pore volumes were calculated with assuming a density of adsorbed  $H_2O$  to be 0.92 g/cm<sup>3</sup>, as suggested by Alcañiz-Monge et al.<sup>32</sup> The last column of Table 1 lists the pore volumes thus calculated from the  $H_2O$  adsorption isotherms. For all cases, each pore volume from the  $H_2O$  isotherm is very close to that from the DR plot of the  $N_2$  isotherm. This finding supports the idea that  $H_2O$  molecules are adsorbed preferentially in micropores.<sup>34</sup> Furthermore, this result indicates that the N doping does not have any significant influence on the saturated amount of  $H_2O$ , but it is controlled only by each micropore volume.

It is noteworthy that the pressure where the rapid  $H_2O$  adsorption took place on A8(2) carbon is lower than that of P7(1) one. In other words, the N-containing porous carbon has stronger affinity to  $H_2O$  than the N-free carbon. Such lower shift of the uptake pressure due to N doping was already reported for ACF and activated carbon.<sup>31,35</sup> It is well-known that the uptake pressure and shape of the  $H_2O$  isotherm are functions of both micropore size and surface chemical properties. However, in our case, we can almost exclude the influence of micropore size and attribute the observed difference in the uptake pressure solely to carbon surface chemistry. It is therefore reasonable to conclude that the inner pore surface of A8(2) carbon is more hydrophilic than that of P7(1) one. Since the O content of the former carbon is lower than that of the latter, the previous results indicate that in our case, the presence of N groups is more effective for  $H_2O$  adsorption. This is partially because the O-functionality in P7(1) carbon is dominated by ether and the amount of more hydrophilic O groups such as carboxyl group is small,<sup>36</sup> as well as the case of A8(2) carbon (Figure 5b). Matsuoka et al. have reported the effectiveness of

- (31) Yang, C.-M.; Kaneko, K. *Carbon* **2001**, *39*, 1075.  
 (32) Alcañiz-Monge, J.; Linares-Solano, A.; Rand, B. *J. Phys. Chem. B* **2002**, *106*, 3209.  
 (33) Mowla, D.; Do, D. D.; Kaneko, K. In *Chemistry and Physics of Carbon*, Vol. 28; Radovic, L. R., Ed.; Marcel Dekker: New York, 2003; p 229.  
 (34) Kaneko, K.; Hanzawa, Y.; Iiyama, T.; Kanda, T.; Suzuki, T. *Adsorption* **1999**, *5*, 7.  
 (35) Cossarutto, L.; Zimny, T.; Kaczmarczyk, J.; Siemieniowska, T.; Bimer, J.; Weber, J. V. *Carbon* **2001**, *39*, 2339.  
 (36) The O-containing functional groups in P7(1) carbon were analyzed by Fourier transform infrared spectroscopy and a temperature-programmed desorption technique.

(30) Hou P.-X.; Yamazaki, T.; Orikasa, H.; Kyotani, T. *Carbon* **2005**, *43*, 2624.

quaternary N in improving water wettability and the promotion of capillary condensation in carbon mesopores as a result.<sup>37</sup> Such function of quaternary N may induce the micropore filling of water molecules at the lower relative pressure into the large micropores of the present carbon. As we described before, there is a slight heterogeneity in N distribution in A8(2) carbon. This may explain why the slope of the adsorption branch in A8(2) carbon is not as sharp as that in P7(1) one. The small but explicit difference in the uptake pressure between the two carbons (P7(1) and P7(1)–A8(0.5)) implies that the N doping has still some effect on the increase in hydrophilicity even though N atoms are present mainly on the carbon outer surface, but the difference between A8(2) and P7(1)–A8(0.5) carbons indicates that the N-doping inside the carbon pore structure is more effective to lower the uptake pressure.

### Conclusions

Nitrogen-containing microporous carbons with ordered periodic structure of zeolite Y were successfully prepared by using zeolite Y as a template. The process of furfuryl alcohol impregnation into zeolite channels followed by acetonitrile CVD was proved to be necessary for preparing

such porous carbons. The optimum CVD (800 °C and 2 h) condition to obtain high structural regularity is the same as that for the development of high microporosity in the carbon structure. The carbon prepared under this condition contains nitrogen of 6 wt %, which is distributed not only on the outer surface of the carbon particles but also in their inside. The BET specific surface area and micropore volume of this carbon reach 3310 m<sup>2</sup>/g and 1.26 cm<sup>3</sup>/g, respectively, but its mesoporosity is low. This carbon is characterized by its very narrow pore size distribution; most of the pore sizes fall within the range of 1.0–1.5 nm. This is the first example for a nitrogen-containing super-high surface area carbon with a narrow micropore size distribution and a highly ordered structure. The H<sub>2</sub>O adsorption–desorption isotherm of this carbon is of Type V, having a steep uptake around  $P/P_0 = 0.5$  and a remarkable hysteresis. Because of the presence of nitrogen atoms, the carbon has a higher affinity to H<sub>2</sub>O molecules than a nitrogen-free porous carbon with a similar microporous and ordered structure.

**Acknowledgment.** This work was partly supported by the Japan Society of Promotion of Science (JSPS) postdoctoral fellowship (P03075) for foreign researchers.

CM051094K

(37) Matsuoka, T.; Hatori, H.; Kodama, M.; Yamashita, J.; Miyajima, N. *Carbon* **2004**, *42*, 2346.